

## Interlayer Dzyaloshinskii-Moriya Interactions

Elena Y. Vedmedenko

*Department of Physics, University of Hamburg, D-20355 Hamburg, Germany*

Patricia Riego

*CIC nanoGUNE, E-20018 San Sebastian, Spain*

*and Departamento de Física de la Materia Condensada, Universidad del País Vasco, UPV/EHU, E-48080 Bilbao, Spain*

Jon Ander Arregi and Andreas Berger

*CIC nanoGUNE, E-20018 San Sebastian, Spain*



(Received 6 April 2018; published 26 June 2019)

The interfacial Dzyaloshinskii-Moriya interaction defines a rotational sense for the spin structure in two-dimensional magnetic films and can be used to create chiral magnetic structures like spin spirals and skyrmions in those films. Here, we show by means of atomistic calculations that in heterostructures an interlayer coupling of the Dzyaloshinskii-Moriya type across a spacer can emerge. We quantify this interaction in the framework of the Lévy-Fert model for trilayers consisting of two ferromagnets separated by a nonmagnetic spacer and show that such an interlayer Dzyaloshinskii-Moriya interaction yields nontrivial three-dimensional spin textures across the entire trilayer, which evolve within as well as between the planes and, hence, combine intraplane and interplane chiralities. This analysis opens new perspectives for three-dimensional tailoring of magnetic chirality in multilayers.

DOI: 10.1103/PhysRevLett.122.257202

The magnetic Dzyaloshinskii-Moriya interaction (DMI) arises in systems with bulk inversion asymmetry [1,2]. Without bulk inversion asymmetry, the DMI arises at interfaces only and couples two magnetic sites both sitting within a surface layer [1,3]. This interaction appeared to be a very important property of interfacial systems because it is responsible for a unique rotational sense of magnetization and can be used to create topological objects like magnetic skyrmions and chiral domain walls [4–7] that are attractive candidates for data storage, transfer, and processing [8–10]. The DMI corresponds to an antisymmetric part

of the exchange tensor and is described by a vector quantity  $\vec{D}$ . The orientation and strength of  $\vec{D}$  can be estimated using the Moriya symmetry rules [11], the Lévy and Fert model [3], or first-principles calculations [12–14]. The Moriya procedure has been created for localized magnetic systems and takes into account two magnetic sites  $i$  and  $j$  coupled by a Hubbard-type Hamiltonian. The Lévy and Fert model is more appropriate for itinerant systems and involves an additional third site  $l$  mediating the DMI via conducting electrons. In this model,

$$\vec{D}_{ijl}(\vec{R}_{li}, \vec{R}_{lj}, \vec{R}_{ij}) = -V_1 \frac{\sin[k_F(|\vec{R}_{li}| + |\vec{R}_{lj}| + |\vec{R}_{ij}|) + (\pi/10)Z_d](\vec{R}_{li} \cdot \vec{R}_{lj})(\vec{R}_{li} \times \vec{R}_{lj})}{|\vec{R}_{li}|^3 |\vec{R}_{lj}|^3 |\vec{R}_{ij}|}, \quad (1)$$

where  $\vec{R}_{li}$ ,  $\vec{R}_{lj}$ , and  $\vec{R}_{ij}$  are the distance vectors between corresponding sites. The parameter  $V_1 = [(135\pi)/32][(\lambda_d \Gamma^2)/(E_F^2 k_F^3)] \sin[(\pi/10)Z_d]$  refers to the material specific quantity defining the DMI strength. with  $k_F$  and  $E_F$  the Fermi wave vector and energy, respectively,  $\lambda_d$  is the spin-orbit coupling parameter,  $\Gamma$  the interaction parameter between the localized spins and the spins of conduction electrons, and  $Z_d$  the number of  $d$  electrons.

Symmetry rules always predict a correct orientation of  $\vec{D}$ . The same is true for the three-sites model in full-symmetry systems. For systems of reduced symmetry,

like chains at interfaces, however, only an easy plane rather than an exact direction of  $\vec{D}$  can be derived from the two-sites model [15], and results of the three-sites model might also differ from *ab initio* results [12]. Nonetheless, it is broadly accepted that for ultrathin films the Lévy-Fert model provides a sound basis for studies of the spin ordering at the interfaces because a majority of experimental  $4d/3d$ ,  $5d/3d$  interfaces or their alloys belong to the class of itinerant systems with large and complicated unit cells.

The typical strength of  $\vec{D}_{ijl}$  at interfaces lies between 0.1 and 2 meV [16–19], which corresponds to the thermal

energy of several tens of kelvin. To enhance the DMI in view of room temperature applications, multilayers of ferromagnetic (FM) and nonmagnetic (NM) metals ..NM1-FM-NM2.. have been proposed [17,20,21]. In these multilayers a strong intralayer and interlayer Rudermann-Kittel-Kasuya-Yoshida (RKKY) coupling was considered, while the DMI was understood to appear within the NM-FM interfaces only. The RKKY coupling ensures collective magnetic behavior of all FM layers. Hence, if the DMI at all interfaces have identical direction, they can be added to enhance the total DMI so that the complete stack exhibits collective behavior. The interlayer DMI across a NM spacer has up to now not been addressed despite the fact that NM atoms or impurities within the NM layer might play a role via the “third site” coupling of magnetic layers. The reason that the interlayer DMI has not been considered yet is, probably, the strong decrease of the DMI with the distance between interacting and mediating sites as shown in Refs. [13,22] and a cancellation of DM vectors for certain symmetries. If, however, the DMI across a spacer exists, different physical scenarios might develop: if the interlayer DMI is supported by the RKKY interlayer coupling, it might further enhance the effective DMI, which could be most relevant for future technological breakthroughs; if the interlayer DMI competes with the RKKY interlayer coupling, some unexpected phenomena like intrinsic separation of columnar skyrmions, bias effects, or three-dimensional frustration might emerge, which would enrich the landscape of possible spin structures, but might also complicate envisioned application scenarios.

In this study, we employ analytical and atomistic Monte Carlo (MC) calculations to investigate the existence and potential properties of DMI coupling between two FM layers across a nonmagnetic spacer. We find that interlayer DMI exists for many microscopic geometries. Despite the weakness of interlayer DMI per atomic bond, it can induce chiral coupling between FM layers, because the total interlayer DM energy creates a sizable energy barrier between macroscopic configurations with different chirality. This coupling is not trivial and seeks to create a three-dimensional spin spiral across the complete system. Therefore, competition between the interlayer DMI and other energy contributions opens a new class of frustrated magnetic systems and can be used to enhance the effective interfacial DMI or to create complex three-dimensional magnetic structures.

In our calculations magnetic layers are represented by monolayers of Heisenberg spins  $\vec{S}_i$  at atomic positions  $\vec{R}_i$  (see Fig. 1). The two effective FM monolayers are separated by a NM metallic layer. The distance between the bottom FM layer and the NM layer is  $d_{\text{NM}}$ . This NM layer is assumed to contain a certain distribution of impurity atoms at positions  $\vec{R}_l$ , which can each mediate a DMI between any two spins according to Eq. (1). This sum is oscillating and, hence, nontrivial. However, for

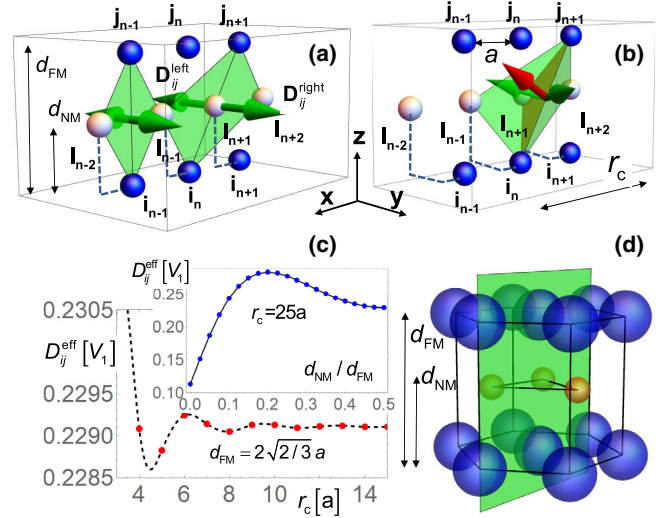


FIG. 1. Microscopic interlayer DM vectors in a trilayer cross-section. (a),(b) Contributions to the  $\vec{D}_{ij}$  (arrows) due to mediating NM sites to the right  $\vec{D}_{ij}^{\text{right}}$  and to the left  $\vec{D}_{ij}^{\text{left}}$  from the bond (green triangles). In (a), magnetic (blue spheres) and nonmagnetic (gray spheres) atoms lie in the same plane and  $\vec{D}_{ij}^{\text{left}} = -\vec{D}_{ij}^{\text{right}}$  leading to  $D_{ij}^{\text{eff}} = 0$ . In (b), the NM atoms are shifted along the  $y$  axis corresponding to a cross section of a hcp stacking shown in (d). Because of the shift,  $D_{ij}^{\text{eff}} \neq 0$ . (c) Effective  $\vec{D}_{ij}^{\text{eff}}$  for a chain with geometry (b) dependent on the number  $n$  of mediating NM atoms ( $r_c = an$ ). The inset displays the dependency of  $D_{ij}^{\text{eff}}$  as a function of the NM atom chain location along the  $z$  axis ( $d_{\text{NM}}$ ) for a given  $d_{\text{FM}}$  and  $r_c = 15a$ . (d) Cross section of a hcp stacking scenario.

typical  $d_{\text{FM}}$ , the sine term is close to unity [23]. An effective DM vector of a given  $ij$  atomic pair can be described by a sum over all impurities  $l$  [3,22]:

$$\vec{D}_{ij}^{\text{eff}} = \sum_l \vec{D}_{ijl}(\vec{R}_{li}, \vec{R}_{lj}, \vec{R}_{ij}). \quad (2)$$

In many one-dimensional cases, individual  $\vec{D}_{ijl}$  are symmetric with respect to any bond and thus add up to zero [arrows in Fig. 1(a)] according to the Eq. (2). A simplest 1D configuration, which is different from that of Fig. 1(a), is displayed in Fig. 1(b). This geometry corresponds to the (1 $\bar{1}$ 00) plane of a hcp structure [Fig. 1(d)] and impurities are shifted in the  $-y$  direction. Because of this shift, the  $\vec{D}_{ijl}$  vectors are not compensated anymore, and hence,  $\vec{D}_{ij}^{\text{eff}}$  becomes nonzero. Figure 1(c) shows strength of  $\vec{D}_{ij}^{\text{eff}}$  according to the geometry shown in Fig. 1(b) as a function of the number of considered  $l$  atoms denoted by the corresponding cutoff radius  $r_c = na$  with  $a$  being the distance between neighboring  $l$  atoms. It shows that  $|\vec{D}_{ij}^{\text{eff}}|$  is maximal ( $\approx 0.231V_1$ ) if only nearest-neighboring impurities are considered, but its value only changes very modestly (to  $\approx 0.229V_1$ ) if further neighbors are taken into

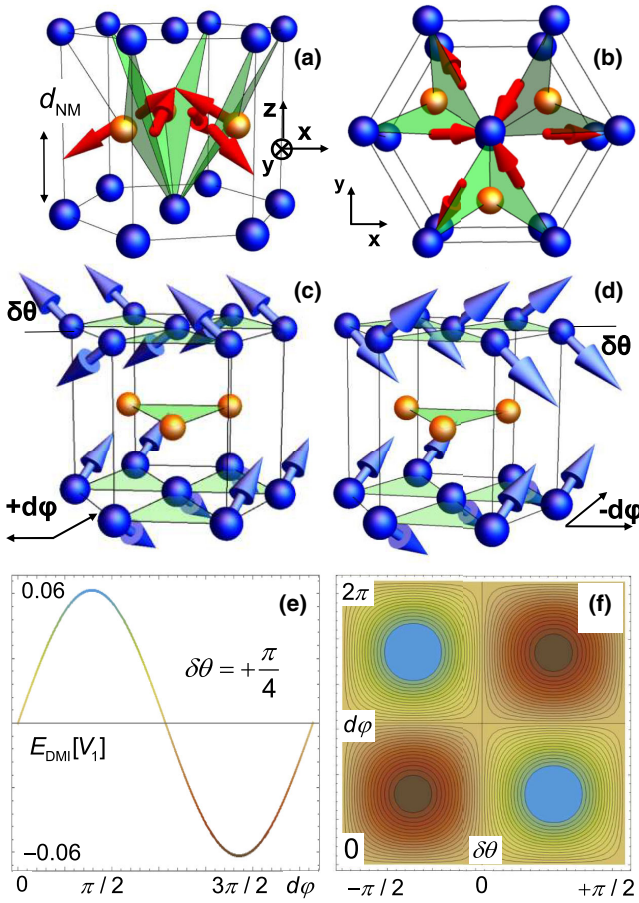


FIG. 2. Interlayer DM energy in a FM-NM-FM trilayer. Calculated orientations of DM vectors in a hcp trilayer for nearest-neighboring mediating atoms: (a) side view and (b) top view. Triangles define the  $ijl$  planes, dark spheres show magnetic atoms, and light spheres correspond to mediating atoms. (c),(d) Blue arrows represent magnetic moments. Energy minimized azimuthal rotations [ $d\varphi = +\pi/2$  in (c) and  $d\varphi = -\pi/2$  in (d)] of the top FM layer with respect to the bottom FM layer for in-phase (c) and antiphase (d)  $\delta\theta$  magnetization oscillations in the top layer (with respect to the bottom layer oscillations). (e),(f) Energy landscape in the  $d\varphi, \delta\theta$  phase space. The exemplary curve for  $\delta\theta = +\pi/4$  in (e) defines the color code of (f).

account. The dependence  $|\vec{D}_{ij}^{\text{eff}}| = f(d_{\text{NM}})$  [see inset of Fig. 1(c)] shows the variation of  $|\vec{D}_{ij}^{\text{eff}}|$  with the position of the NM layer along the  $z$  axis. The calculated  $\vec{D}_{ij}^{\text{eff}}$  for a complete hcp unit cell are shown in Figs. 2(a) and 2(b).

To calculate the total DM energy for an FM-NM-FM trilayer with hcp stacking [see Figs. 2(a) and 2(b)], we use the standard expression:

$$E_{\text{DM}} = \sum_{ij} \vec{D}_{ij}^{\text{eff}} \cdot (\vec{S}_i \times \vec{S}_j). \quad (3)$$

First, we analyze  $E_{\text{DM}}$  for the case in which FM1 and FM2 are each characterized by a perfectly aligned ferromagnetic state, but allowed to have any orientation with respect to one another. Because in this case the spin cross

product is identical and constant for all pairs, the DM energy per site is

$$E_{\text{DM}}^i = (\vec{S}_i \times \vec{S}_j) \cdot \sum_j \vec{D}_{ij}^{\text{eff}}. \quad (4)$$

While individual  $\vec{D}_{ij}^{\text{eff}}$  are nonvanishing, their sum  $\sum_j \vec{D}_{ij}^{\text{eff}}$  vanishes, because all  $\vec{D}_{ij}^{\text{eff}}$  for a site  $i$  in a hexagon cancel out, as can be seen in Figs. 2(a) and 2(b). In other words,  $E_{\text{DM}}$  cannot be minimized even if nonzero  $\vec{D}_{ij}^{\text{eff}}$  exist. However, if magnetization configurations exhibit deviations from perfect ferromagnetic alignment, the spin cross product cannot be taken out of the sum and indices of the two vectors cannot be separated. Hence, Eq. (3) cannot be converted into the simple form of Eq. (4). Instead, spin and distance variables become mixed and the total  $E_{\text{DMI}}$  might become nonzero.

To illustrate this we conduct a simplified analytical minimization of the total DM energy calculated on the basis of Eq. (3) with respect to some particular noncollinear spin states. For this, we assume that azimuthal spin angles  $\varphi_i$  within each FM layer are identical, while  $\varphi_i^{\text{FM1}}$  and  $\varphi_i^{\text{FM2}}$  can take any values. We furthermore assume row-wise up-down deviations of identical magnitude  $\pm\delta\theta$  of spins from  $\theta = \pi/2$ , as visualized in Figs. 2(c) and 2(d). We have, however, distinguished between in-phase (up-up, down-down) and antiphase (up-down, down-up) polar oscillations. By applying these constraints we simplify the problem and reduce the system to having two state variables ( $\delta\theta$  and  $d\varphi = \varphi_i^{\text{FM2}} - \varphi_i^{\text{FM1}}$ ) only. Figures 2(e) and 2(f) show the analytically calculated interlayer  $E_{\text{DM}}$  as a function of  $d\varphi$  and  $\delta\theta$  for these two sequences. The DM energy is minimized by  $\delta\theta = \pi/4$  and  $d\varphi = +3\pi/2$  ( $= -\pi/2$ ) for the in-phase and by  $\delta\theta = \pi/4$  and  $d\varphi = +\pi/2$  for the antiphase sequence [see Figs. 2(c) and 2(d)]. Hence, by considering only the interlayer DM energy term, and despite the fact that we constrain solution space, we find magnetization states that exhibit a net ferromagnetic moment in each of the two FM layers while achieving a net reduction of the DM energy upon rotating the two layer magnetizations with respect to each other following a preferred helicity. This constitutes a DMI interlayer coupling effect.

For the more comprehensive understanding of interlayer DMI coupling, we used Monte Carlo simulations. Samples with lateral dimensions of up to  $30a \times 30a$  with periodic and open boundaries have been considered. We use the hcp stacking presented in Fig. 1(d). The magnetic Hamiltonian,

$$H = - \sum_{\langle ij \rangle} J_{ij}^{\text{intra}} (\vec{S}_i \cdot \vec{S}_j) + K_{xy}^i \sum_i (S_i^z)^2 - \sum_{\langle ij \rangle} \vec{D}_{ij}^{\text{eff}} \cdot (\vec{S}_i \times \vec{S}_j), \quad (5)$$

includes ferromagnetic intralayer Heisenberg exchange coupling  $J_{ij}^{\text{intra}}$ , interlayer DM interactions  $\vec{D}_{ij}^{\text{eff}}$  [according to Eq. (2)], as well as an easy-plane  $K_{xy}^i$  anisotropy to mimic magnetostatic effects. First, we set to zero all

contributions except that of  $\vec{D}_{ij}^{\text{eff}}$  calculated for each pair using Eq. (3) (see Ref. [24]). The corresponding ground state of the energy of  $\langle E_{\text{DM}} \rangle \approx -0.82V_1/\text{atom}$  is depicted in Fig. 3(a). It is an antiferromagnetic (AFM) row-wise ordering in both layers. Hereby, magnetization in one of the layers is perpendicular to the film plane, while the other is planar. The total state demonstrates clockwise cycloidal spin spiral across both layers [dark path in Fig. 3(a)] and clockwise cycloidal rotation between the layers. Hence, unique chirality between the layers and a unique AFM modulation within the layers define a unique magnetic chirality across the layers. This nontrivial structure is different from a typically one-dimensional bulk spin spiral with perfect FM order in each plane. Next, we add FM intralayer exchange interaction. For dominating  $D_{ij}^{\text{eff}}/J_{ij}^{\text{intra}} > 1.4$ , the ground state remains the same, while for weaker  $D_{ij}^{\text{eff}}/J_{ij}^{\text{intra}}$  values the AFM stripes broaden and acquire noncollinearity, which is a necessary condition for nonvanishing interlayer coupling [Fig. 3(b)].

One of the key purposes of our study is to investigate whether the interlayer DMI can occur and cause chirality in the in-plane multilayers. To mimic these structures with dominating intralayer Heisenberg exchange and force their magnetization into the film plane, we add an easy-plane anisotropy and use parameters typical for Co-based alloys [25]:  $J_{ij}^{\text{intra}} = 10$  meV per atomic bond,  $D_{ij}^{\text{eff}} \approx 0.025J_{ij}^{\text{intra}}$ , and shape anisotropy  $K_{xy}^{\text{top}} = 0.15J_{ij}^{\text{intra}}$ . An additional small uniaxial in-plane anisotropy in the bottom plane  $K_{[1\bar{1}20]}^{\text{bot}}$  gives a preferential in-plane orientation to make the resulting magnetic state more stable and, thus, the study more transparent overall. Typical stable magnetic states are analyzed in Figs. 3(b)–3(d). Net in-plane magnetization in both layers is close to unity, while  $S_z$  varies between  $+0.1$  and  $-0.1$ . The MC ground state obtained after slow cooling from a random initial configuration with open boundary conditions [24] is shown in the bottom inset of Fig. 3(b). We find a helicoidal rotation of the two FM layers, which indicates interlayer DM coupling.

To clarify the physical grounds of this chirality, we have performed additional computations. Specifically, we started MC simulations using perfect in-plane ferromagnetic states in each layer making an angle  $d\phi$  with respect to one another as initial configuration and relaxed these states at low temperature ( $kT < D_{ij}^{\text{eff}}$ ) until the DM energy started to oscillate around the minimum mean value associated with this macroscopic magnetization orientation. Hereby, azimuthal spin angles were fixed, while polar angles were free to relax. The lateral spin structure acquired out-of-plane modulations leading to DM energy lowering in each case, meaning that the data represent local energy minima that are constrained by the net macroscopic orientation. Obtained mean energies  $\langle E_{\text{DM}} \rangle$  for different  $d\phi$  are plotted in Fig. 3(c). One global and one local energy minima were observed. The global energy minimum corresponds to the clockwise  $\pi/2$  rotation of the top layer with respect to the

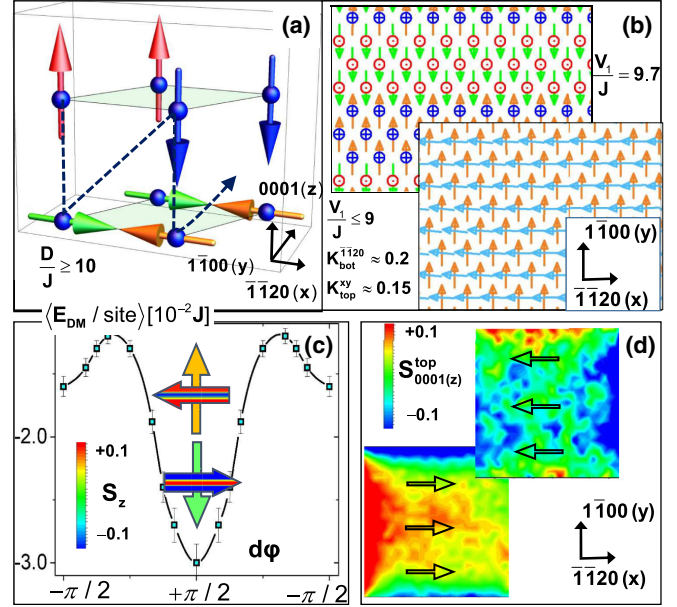


FIG. 3. Ground states of trilayers with interlayer DM interaction from MC simulations. (a) Unit cell of stable MC low-temperature ( $k_B T = 0.001 J_{ij}^{\text{intra}}$ ) configuration for dominating interlayer DM ( $|\vec{D}_{ij}^{\text{eff}}| > J_{ij}^{\text{intra}}$ ). Cycloidal spin spirals across the trilayer (dark dashed line) and along the  $z$  axis are formed. (b) Top view of the magnetic structure for  $D_{ij}^{\text{eff}}/J_{ij}^{\text{intra}} \approx 1.4$  ( $V_1/J_{ij}^{\text{intra}} = 9.7$ ) with the same color scale (blue and red correspond to opposite out-of-plane magnetization, while green and orange correspond to opposite in-plane magnetization) and realistic case  $D_{ij}^{\text{eff}}/J_{ij}^{\text{intra}} \approx 0.15$ . In the last case both layers are in-plane magnetized (cyan and orange spins have orthogonal orientation). (c) Mean interlayer DM energy achieved in MC simulations for net in-plane ferromagnetic states in each layer making an angle  $d\phi$  with respect to one another. Large arrows schematize MC states at the energy minimum. Direction gives net in-plane orientation, color gives an out-of-plane contrast. (d) Stable MC low-temperature ( $k_B T = 0.001 J_{ij}^{\text{intra}}$ ) configurations of the top layer for  $D_{ij}^{\text{eff}}/J_{ij}^{\text{intra}} \approx 0.2$ , and  $K_{xy}^{\text{top}} = 0.15 J_{ij}^{\text{intra}}$  for  $d\phi = +\pi/2$ . Arrows show net in-plane orientation, while colors show the out-of-plane magnetic contrast.

bottom one, while the local energy minimum corresponds to an anticlockwise rotation. The local minimum appears due to the open boundaries. The out-of-plane modulation [see Fig. 3(d)] always inherited the chirality across the trilayer from the pure DM ground state [Fig. 3(a)]. For instance, if the bottom layer is magnetized in the  $+y$  direction (orange arrows), the top layer acquires an up state with decreasing its vertical component towards the sample rim (down-up-down) in conjunction with its net orientation to the left; if the bottom layer is oriented along the  $-y$  axis (green arrows), the modulation and net orientation of the top layer is reversed. Hence, the interlayer DMI for in-plane magnetic bilayers with dominating exchange interactions can lead to a unique interlayer chirality combined with specific and associated  $S_z$  modulation: the change of the

sign in chirality requires a sign change in the phase of out-of-plane modulations and vice versa.

The strength of the interlayer DM energy in planar bilayers is, according to our calculations, of the order of  $10^{-2}J_{ij}$  per atom. While the interlayer DM cannot compete with strong Heisenberg exchange at the atomic scale, it can define the energy barrier between two global configurations with different relative magnetization orientations of individual layers because it scales with the sample size. Specifically, this energy barrier is given by the total  $\langle E_{DM}^{\text{inter}} \rangle \approx J_{ij}$  in a sample consisting of  $2 \times 10^3$  spins for our specific boundary conditions and, therefore, can shape the resulting equilibrium state. We expect an important impact of this interlayer DMI causing three-dimensional chirality of magnetic multilayers like Fe/Cr/Fe [26], Co/Cu/Co [27], Co/Ru/Co [28], Fe/Mo/Fe [29], and related Co or Fe alloys like Co/Pt/CoFeB or CoFeB/Ru/CoFeB [20,30]. The interlayer DMI is probably responsible for the spin canting in Fig. 3 of Ref. [31]. The strength of the resulting interlayer DMI should be controllable by means of the thickness and atomic structure of the NM layer.

The main conclusion of this investigation is that in addition to the now well-explored interfacial DMI, magnetic layers can be strongly coupled by means of a so-far neglected interlayer DM interaction across a mediating layer. The driving mechanism of this interlayer DM coupling is the formation of a global chiral structure across magnetic multilayers in all spatial directions (in plane and out of plane), which is significantly different from a one-dimensional bulk spin spiral. In ferromagnetic systems, a given phase of microscopic deviations from collinearity defines the sign of the interlayer chirality. Our findings open completely new perspectives for enhancement and/or manipulation of the total DM interaction and magnetic structuring in magnetic multilayers because the interlayer DMI might compete with the interfacial DMI and the oscillatory interlayer exchange coupling often present in multilayers. This competition might lead to novel phenomena like chiral exchange bias [32]. The microscopic characteristics of this interaction depend on the lattice geometry of FM-NM-FM stacks, on the strength of the spin-orbit coupling parameter  $V_1$ , and on the lateral structure of the films.

[1] A. Fert, *Mater. Sci. Forum* **59–60**, 439 (1990).

[2] A. Bogdanov and A. Hubert, *Phys. Status Solidi B* **186**, 527 (1994).

[3] P. M. Lévy and A. Fert, *Phys. Rev. B* **23**, 4667 (1981).

[4] S. Heinze, K. von Bergmann, M. Menzel, J. Brede, A. Kubetzka, R. Wiesendanger, G. Bihlmayer, and S. Blügel, *Nat. Phys.* **7**, 713 (2011).

[5] J. Sampaio, V. Cros, S. Rohart, A. Thiaville, and A. Fert, *Nat. Nanotechnol.* **8**, 839 (2013).

[6] N. Romming, A. Kubetzka, C. Hanneken, K. von Bergmann, and R. Wiesendanger, *Phys. Rev. Lett.* **114**, 177203 (2015).

[7] S. Woo, K. Litzius, B. Krüger, M. Im, L. Caretta, K. Richter, M. Mann, A. Krone, R. Reeve, M. Weigand *et al.*, *Nat. Mater.* **15**, 501 (2016).

[8] S.-Z. Lin, C. Reichhardt, and A. Saxena, *Appl. Phys. Lett.* **102**, 222405 (2013).

[9] N. S. Kiselev, A. Bogdanov, R. Schäfer, and U. K. Rössler, *J. Phys. D* **44**, 392001 (2011).

[10] A. Fert, V. Cros, and J. Sampaio, *Nat. Nanotechnol.* **8**, 152 (2013).

[11] T. Moriya, *Phys. Rev.* **120**, 91 (1960).

[12] B. Schweflinghaus, B. Zimmermann, M. Heide, G. Bihlmayer, and S. Blügel, *Phys. Rev. B* **94**, 024403 (2016).

[13] H. Yang, A. Thiaville, S. Rohart, A. Fert, and M. Chshiev, *Phys. Rev. Lett.* **115**, 267210 (2015).

[14] L. Udvardi, L. Szunyogh, K. Palotás, and P. Weinberger, *Phys. Rev. B* **68**, 104436 (2003).

[15] A. Crépieux and C. Lacroix, *J. Magn. Magn. Mater.* **182**, 341 (1998).

[16] M. Heide, G. Bihlmayer, and S. Blügel, *Phys. Rev. B* **78**, 140403(R) (2008).

[17] B. Dupé, G. Bihlmayer, S. Blügel, and S. Heinze, *Nat. Commun.* **7**, 11779 (2016).

[18] J. Hagemester, N. Romming, K. von Bergmann, E. Y. Vedmedenko, and R. Wiesendanger, *Nat. Commun.* **6**, 8455 (2015).

[19] L. Rózsa, L. Udvardi, L. Szunyogh, and I. A. Szabó, *Phys. Rev. B* **91**, 144424 (2015).

[20] C. Moreau-Luchaire, C. Moutafis, N. Reyren, J. Sampaio, C. A. F. Vaz, N. V. Horne, K. Bouzehouane, K. Garcia, C. Deranlot, P. Warnicke *et al.*, *Nat. Nanotechnol.* **11**, 444 (2016).

[21] S. P. Kang, N. J. Kim, H. Y. Kwon, J. W. Choi, B. C. Min, and C. Won, *Sci. Rep.* **8**, 2361 (2018).

[22] S. Tacchi, R. E. Troncoso, M. Ahlberg, G. Gubbiotti, M. Madami, J. Akerman, and P. Landeros, *Phys. Rev. Lett.* **118**, 147201 (2017).

[23] Using  $k_F = 0.875 \text{ \AA}^{-1}[\text{Co/Pt}(111)] - 1.36 \text{ \AA}^{-1}(\text{CuMnT})$  and  $Z_d = 7(\text{Co}) - 9.6(\text{Pt})$ , the sin term is  $\sin[k_F(R_{li} + R_{lj} + R_{ij}) + (\pi/10)Z_d] \approx 0.8 - 0.999$ .

[24] See Supplemental Material at <http://link.aps.org/supplemental/10.1103/PhysRevLett.122.257202> for a discussion and figures that illustrate used boundary conditions and provide calculation details of effective Dzyaloshinskii-Moriya vectors.

[25] C. Eyrich, W. Huttema, M. Arora, E. Montoya, F. Rashidi, C. Burrowes, B. Kardasz, E. Girt, B. Heinrich, O. N. Mryasov *et al.*, *J. Appl. Phys.* **111**, 07C919 (2012).

[26] P. Grünberg, R. Schreiber, Y. Pang, M. B. Brodsky, and H. Sowers, *Phys. Rev. Lett.* **57**, 2442 (1986).

[27] S. S. P. Parkin, R. Bhadra, and K. P. Roche, *Phys. Rev. Lett.* **66**, 2152 (1991).

[28] S. S. P. Parkin, N. More, and K. P. Roche, *Phys. Rev. Lett.* **64**, 2304 (1990).

[29] Z. Q. Qiu, J. Pearson, A. Berger, and S. D. Bader, *Phys. Rev. Lett.* **68**, 1398 (1992).

[30] N. Wiese, T. Dimopoulos, M. Ruhrig, J. Wecker, H. Brueckl, and G. Reiss, *Appl. Phys. Lett.* **85**, 2020 (2004).

[31] S. Blizak, G. Bihlmayer, S. Blügel, and S. E. H. Abaidia, *Phys. Rev. B* **91**, 014408 (2015).

[32] A. Fernandez-Pacheco, E. Y. Vedmedenko, F. Ummelen, R. Mansell, D. Petit, and R. P. Cowburn, [arXiv:1810.01801](https://arxiv.org/abs/1810.01801).